Supplement of Earth Syst. Dynam., 13, 1437–1450, 2022
https://doi.org/10.5194/esd-13-1437-2022-supplement

Earth System Dynamics
Open Access
EGU

Supplement of

Constraining low-frequency variability in climate projections to predict climate on decadal to multi-decadal timescales – a poor man's initialized prediction system

Rashed Mahmood et al.

Correspondence to: Rashed Mahmood (rashed.mahmood@bsc.es)

Table S1: CMIP6 model simulations used in this study.

Model	Institution	# of DCPP-A members	# of unconstrained members	Reference
ACCESS-CM2	CSIRO-ARCCSS	-	3	Bi et al. (2020)
ACCESS-ESM1-5	CSIRO	-	6	Ziehn et al. (2020)
BCC-CSM2-MR	BCC	8	1	Wu et al. (2019)
CAMS-CSM1-0	CAMS	-	2	Rong et al. (2019)
CAS-ESM2-0	CAS	-	2	Guangqing et al. (2020)
CESM2	NCAR	-	1	Danabasoglu et al. (2020)
CESM2-WACCM	NCAR	-	3	Gettelman et al. (2019)
CMCC-CM2-SR5	CMCC	6	1	Cherchi et al. (2019)
CMCC-ESM2	CMCC	-	1	Lovato et al. (2022)
CanESM5	CCCma	20	25	Swart et al. (2019)
CanESM5-CanOE	CCCma	-	3	Christian et al. (2022)
CNRM-CM6-1	CNRM-CERFACS	-	6	Voldoire et al. (2019)
CNRM-CM6-1-HR	CNRM-CERFACS	-	1	Voldoire et al. (2019)
CNRM-ESM2-1	CNRM-CERFACS	-	10	Séférian et al. (2019)
EC-Earth3	EC-Earth consortium	10	13	Bilbao et al. (2021)
FGOALS-f3-L	CAS	-	1	He et al. (2019)
FGOALS-g3	CAS	-	3	Pu et al. (2020)
FIO-ESM-2-0	FIO-QLNM	-	3	Bao et al. (2020)
GISS-E2-1-G	NASA-GISS	-	10	Kelley et al. (2020)
HadGEM3-GC31-LL	MOHC	-	1	Andrews et al. (2020)
HadGEM3-GC31-MM	MOHC	10	-	Sellar et al. (2020)
IITM-ESM	CCCR-IITM	-	1	Krishnan et al. (2019)
INM-CM5-0	INM	-	1	Volodin et al. (2017)
IPSL-CM6A-LR	IPSL	10	11	Boucher et al. (2020)
KIOST-ESM	KIOST	-	1	Pak et al. (2021)
MIROC-ES2L	MIROC	-	30	Hajima et al. (2020)
MIROC6	MIROC	10	50	Tatebe et al. (2019)
MPI-ESM1-2-HR	MPI-M	9	-	Müller et al. (2018)

MPI-ESM1-2-LR	MPI-M	-	10	Mauritsen et al. (2019)
MRI-ESM2-0	MRI	-	1	Yukimoto et al. (2019)
NESM3	NUIST	-	2	Cao et al. (2018)
NorESM2-LM	NCC	-	3	Seland et al. (2020)
NorESM2-MM	NCC	-	1	Seland et al. (2020)
NorCPM1	NCC	10	-	Bethke et al. (2021)
UKESM1-0-LL	NIMS-KMA	-	5	Sellar et al. (2019)

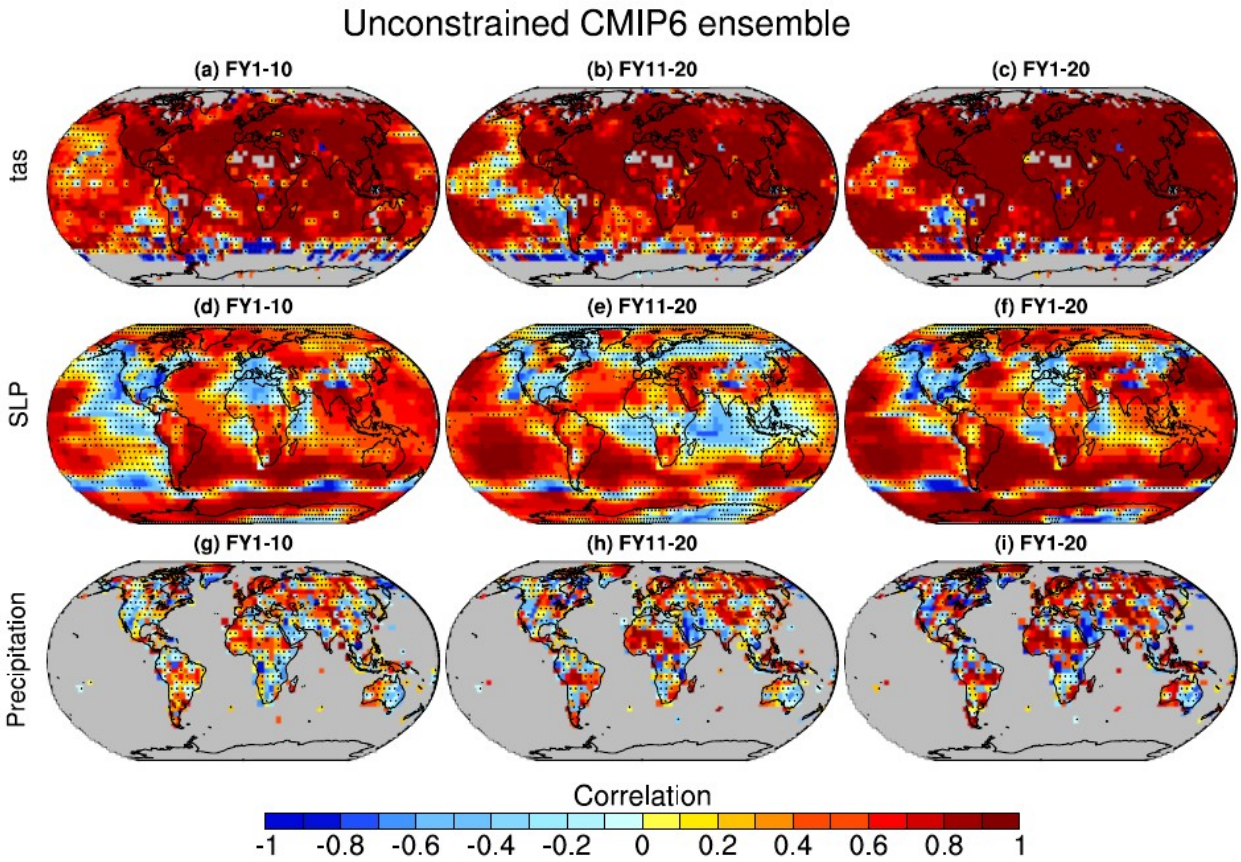

Figure S1: ACC of the unconstrained CMIP6 ensemble mean for near-surface temperature (a-c), SLP (d-f), and precipitation (g-i). Stipplings indicate regions where the results are statistically not significant at 95% confidence level.

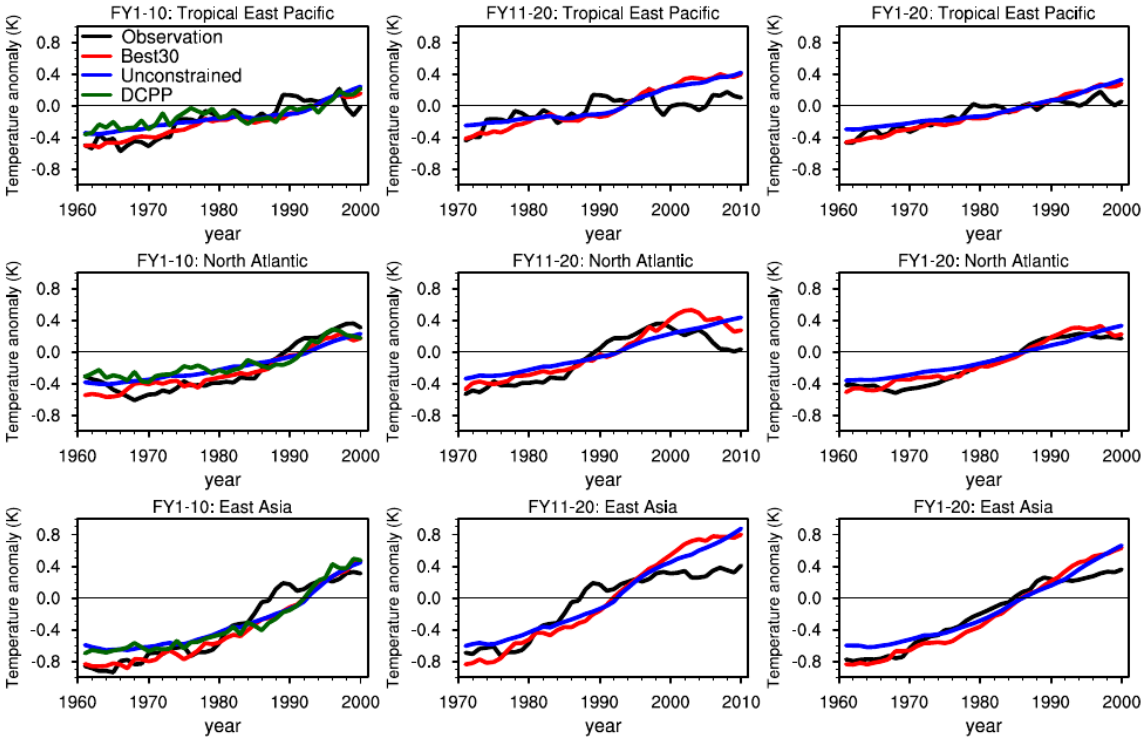

Figure S2: Time-series of area weighted regional averages of surface temperature anomalies (relative to the 1981-2010 mean) over the tropical eastern Pacific (5°S-5°N, 120°W-80°W) in the top row, north Atlantic (35°N-55°N, 45°W-25°W) in the middle row, and east Asia (35°N-65°N, 105°E-145°E) in the bottom row. Best30 is constrained by 9 year mean global SST anomalies. The years on the x-axis represent the first year of the respective 10 or 20 year forecasting periods.

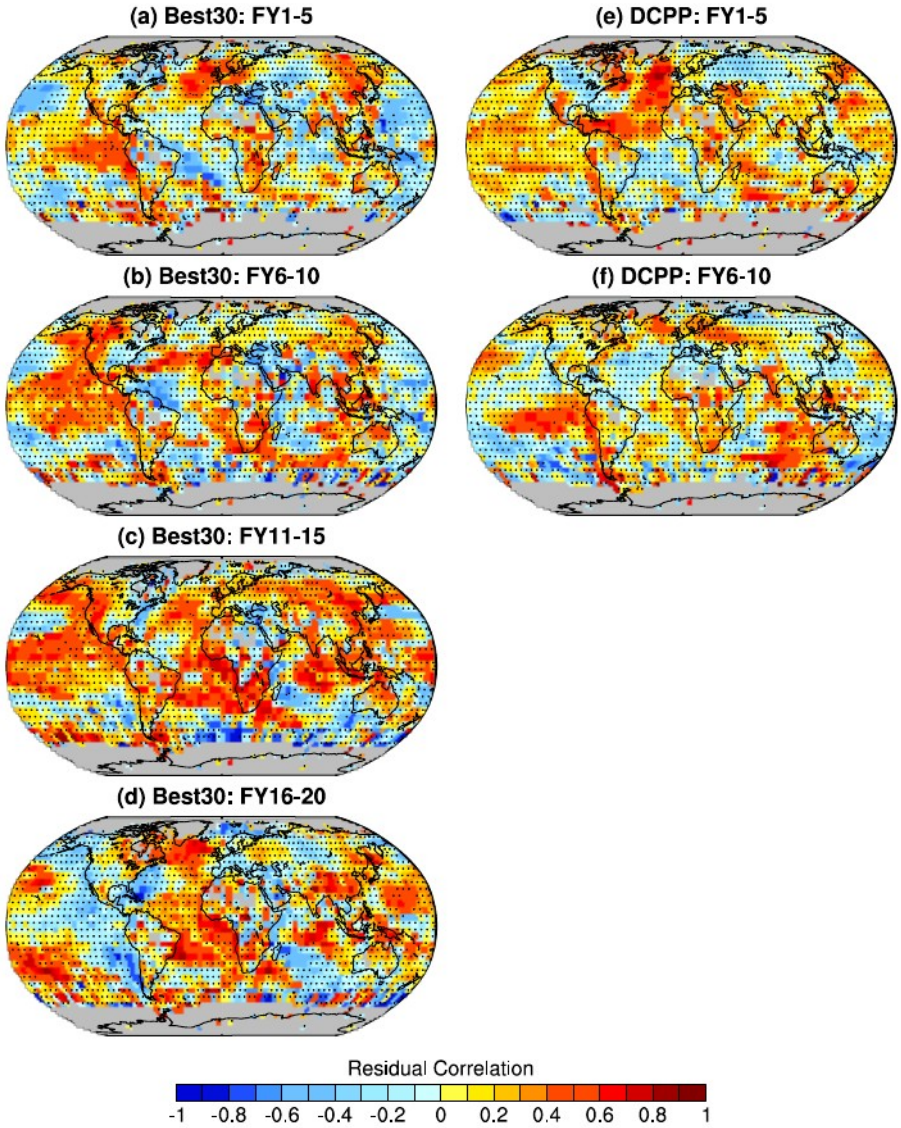

Figure S3: Residual correlations after removing the forced signal (estimated based on ensemble mean of the unconstrained 212 members following Smith et al. (2019)) for near-surface temperature in the Best30 ensemble mean (a-d) and DCPP ensemble mean (e-f). The Best30 ensemble is constrained by 9 year average SST anomaly patterns. Stipplings indicate regions where the results are statistically not significant at 95% confidence level.

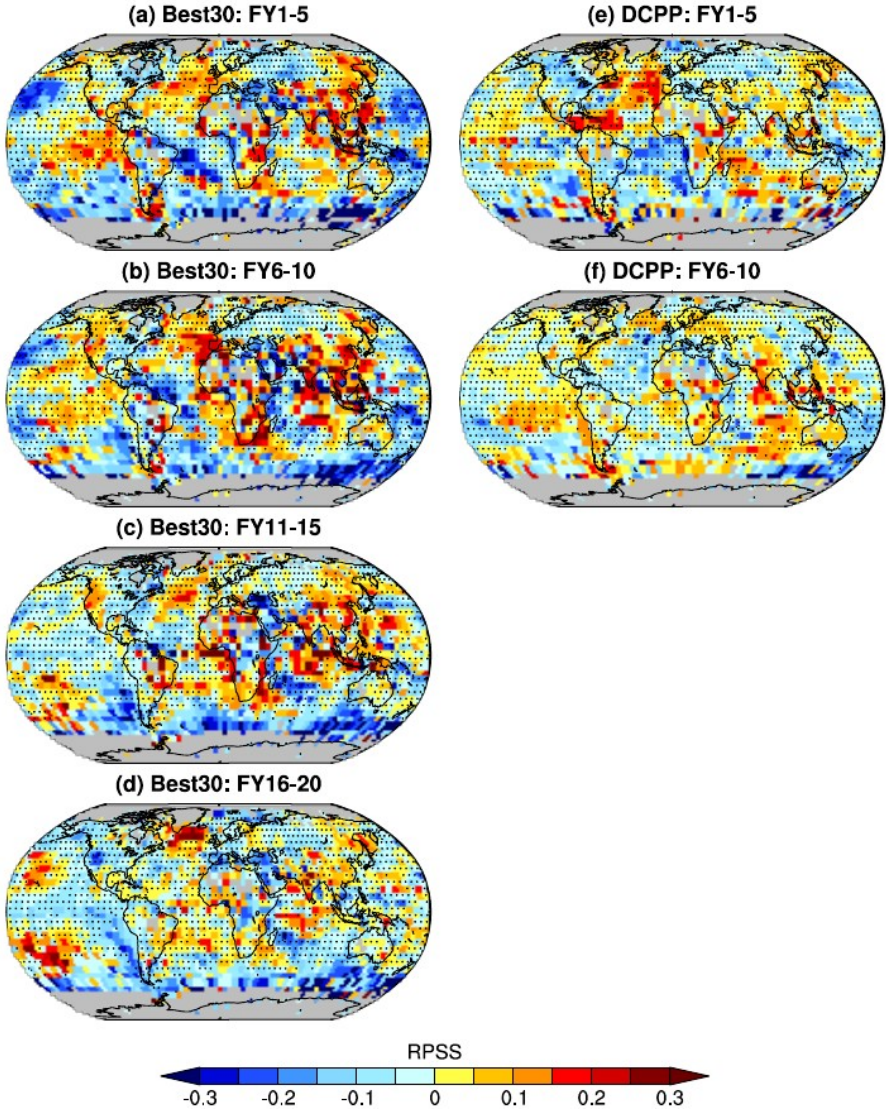

Figure S4: RPSS for near-surface temperature in the Best30 ensemble mean (a-d) and DCPP ensemble mean (e-f) against the unconstrained CMIP6 ensemble of 212 members as reference. The Best30 ensemble is constrained by 9 year average SST anomaly patterns. Stipplings indicate regions where the results are statistically not significant at 95% confidence level.

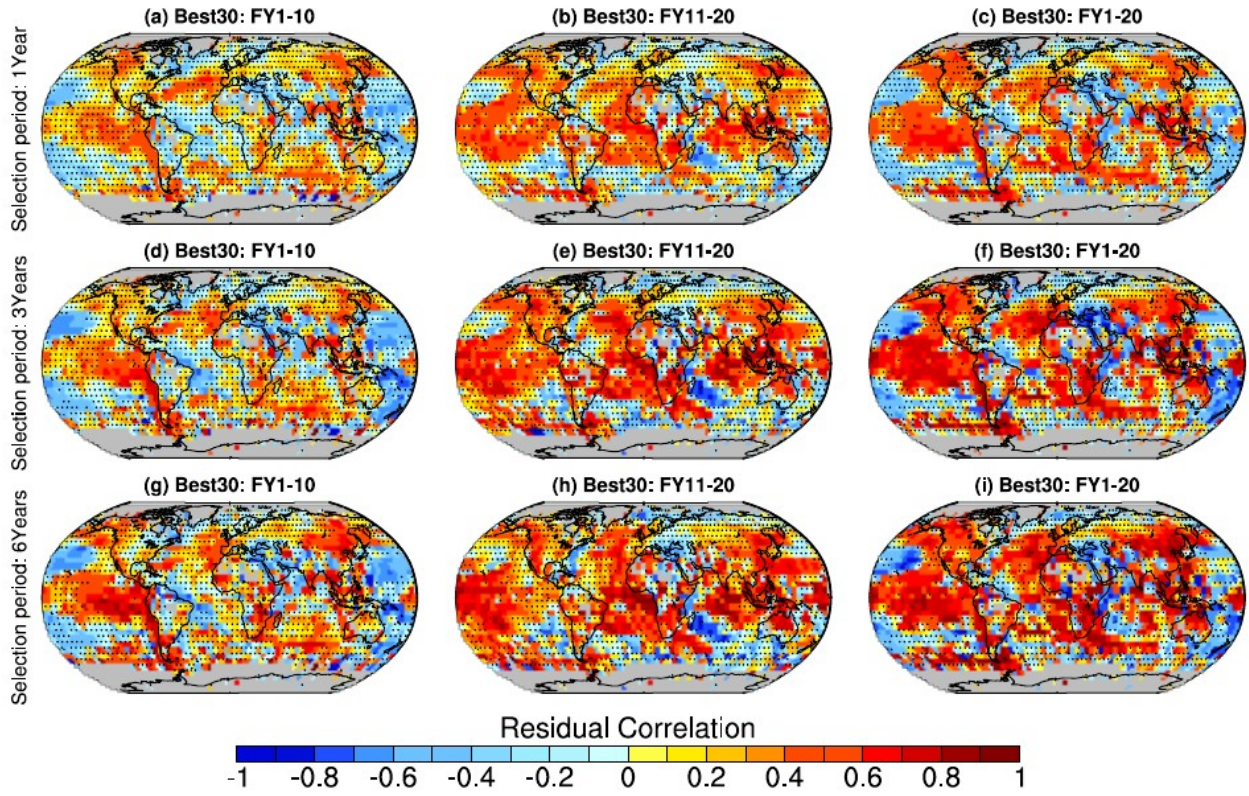

Figure S5: Residual correlations for near-surface temperature in the Best30 ensemble means after removing the forced signal (estimated based on ensemble mean of the unconstrained 212 members following Smith et al. (2019)). The Best30 ensemble is constrained by one year average SST anomaly patterns (a-c), three year average SST anomaly patterns (d-f), and six year average SST anomaly patterns (g-i). Stipplings indicate regions where the results are statistically not significant at 95% confidence level.

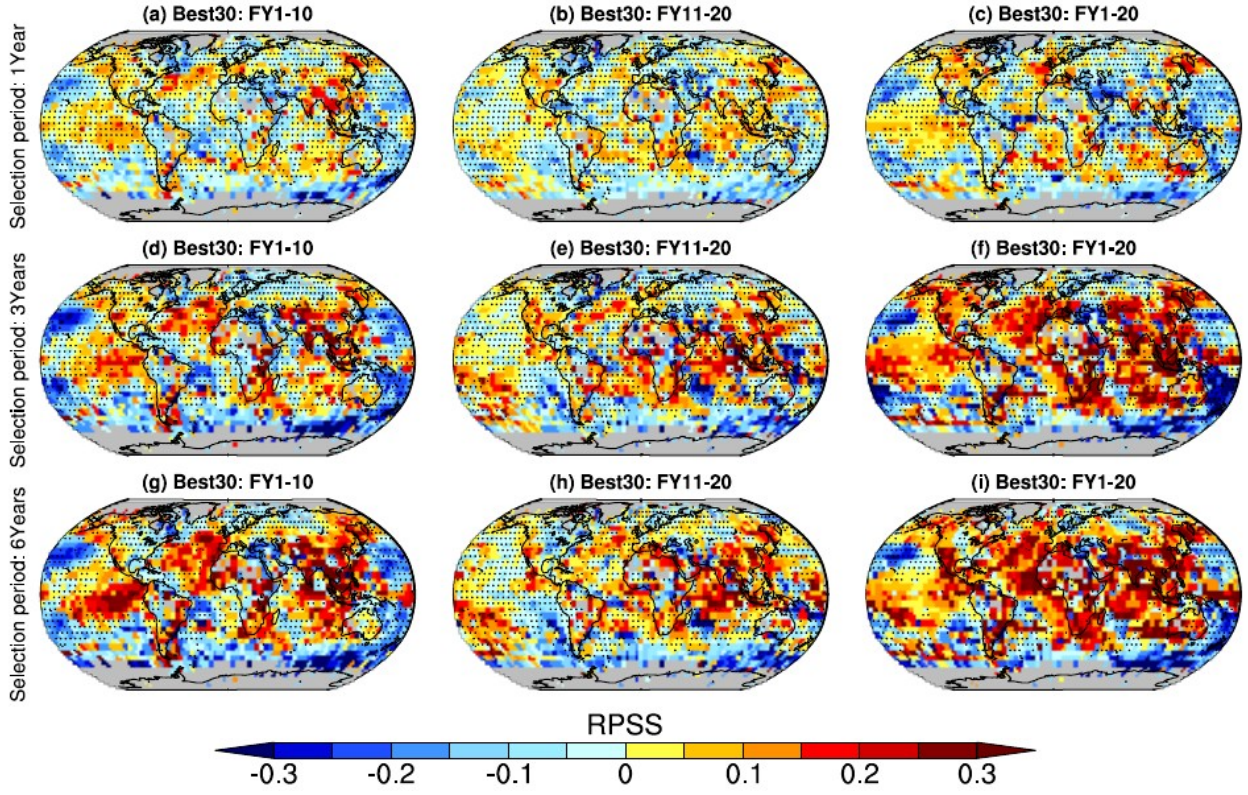

Figure S6: RPSS for near-surface temperature in the Best30 ensemble against the unconstrained CMIP6 ensemble of 212 members as reference. Best30 ensemble is constrained by one year average SST anomaly patterns (a-c), three year average SST anomaly patterns (d-f), and six year average SST anomaly patterns (g-i). Stipplings indicate regions where the results are statistically not significant at 95% confidence level.

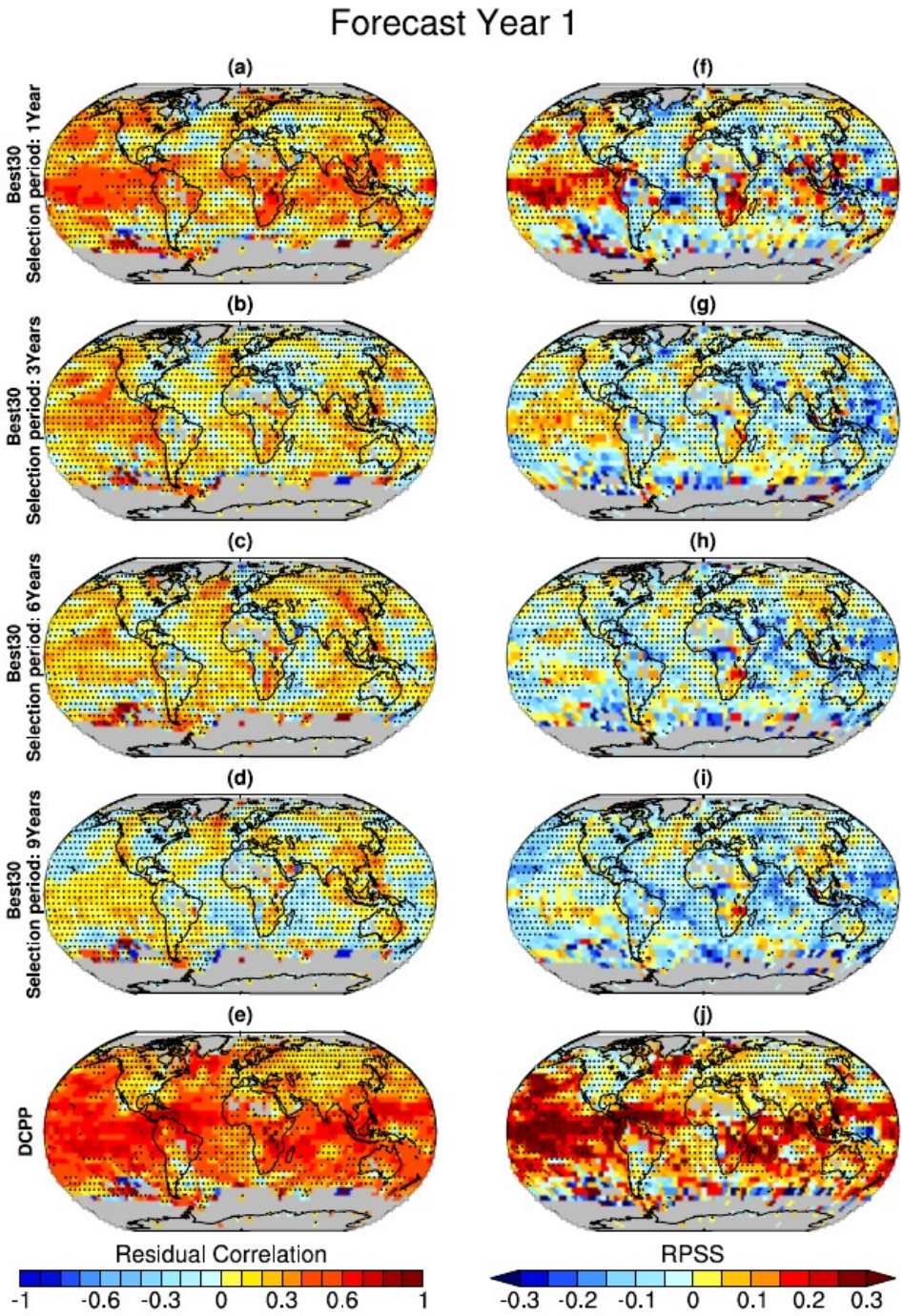

Figure S7: Residual correlation (a-e) and RPSS (f-j) for near-surface temperature in forecast year 1. (a-d) and (f-i) show added value for the Best30 ensemble selected based on SST anomalies of different time periods (i.e. using 1, 3, 6, and 9 year average SST anomaly patterns). (e) and (f) show added value for DCPP. Stipplings indicate regions where the results are statistically not significant at 95% confidence level.

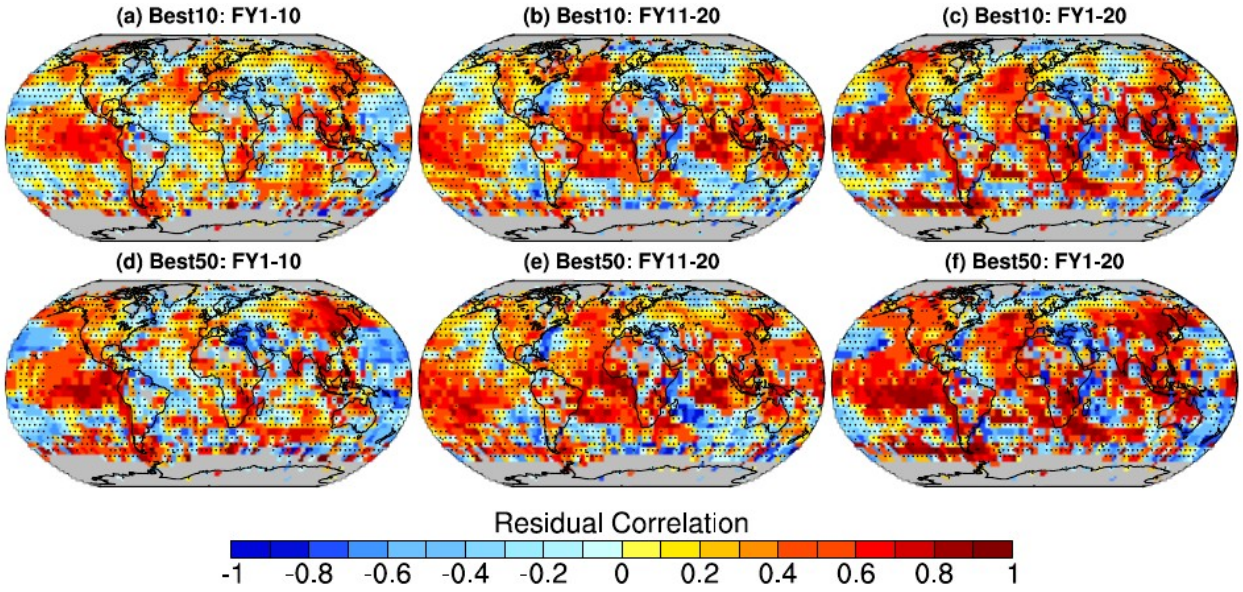

Figure S8: Residual correlations for near-surface temperature in the Best 10 (a-c) and Best50 (d-f) ensemble means constrained by nine year average SST anomaly patterns. Stipplings indicate regions where the results are statistically not significant at 95% confidence level.

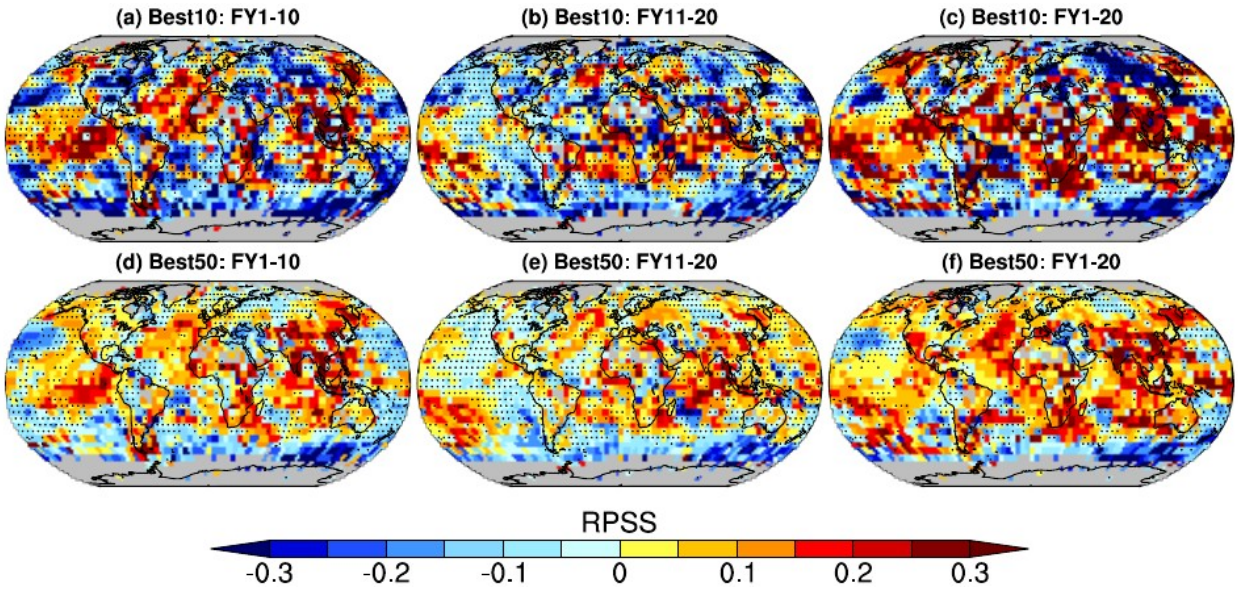

Figure S9: RPSS for Best10 (a-c) and Best50 (d-f) near-surface temperature against the unconstrained CMIP6 ensemble of 212 members as reference. Stipplings indicate regions where the results are statistically not significant at 95% confidence level.

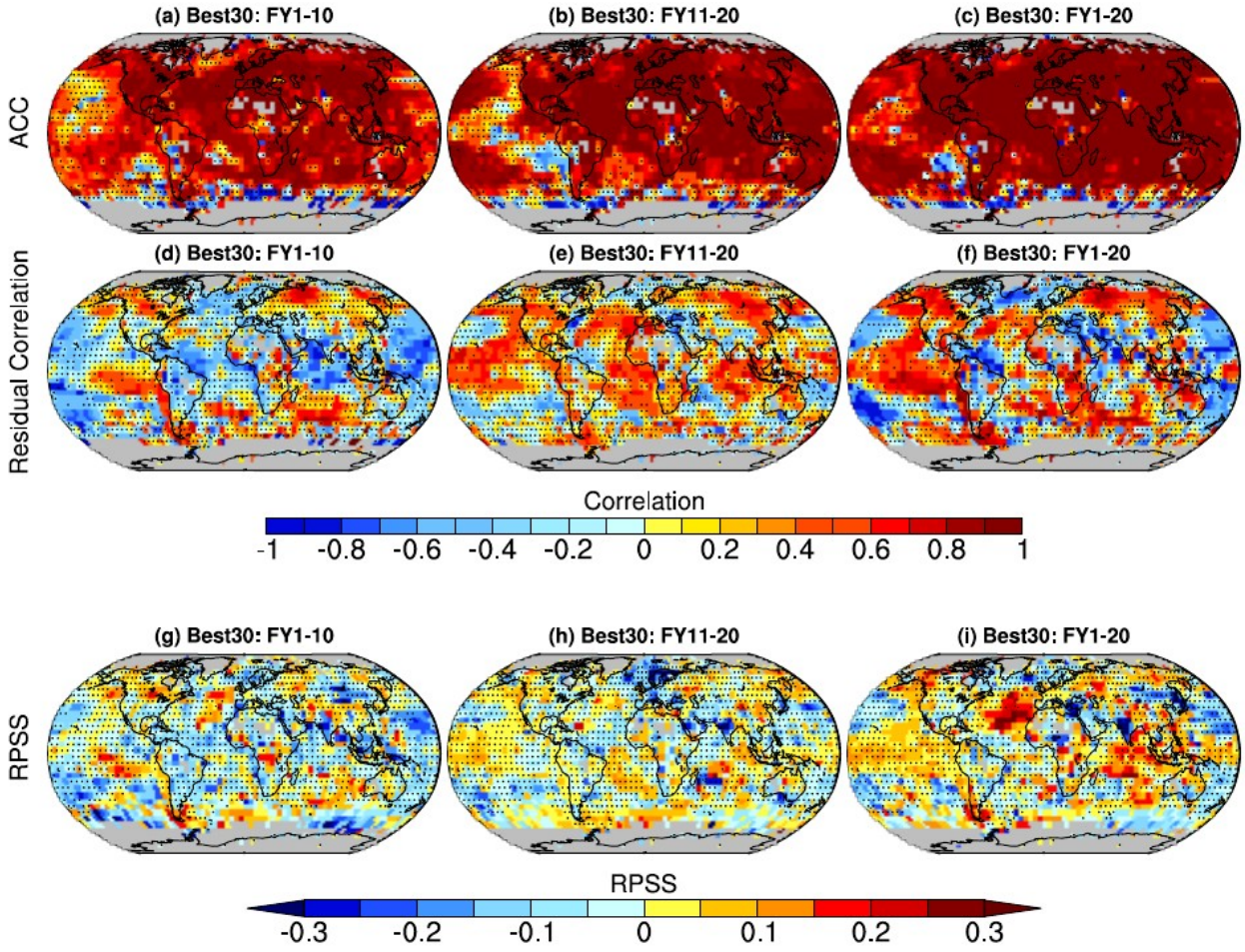

Figure S10: Same as Figure 2 (without DCPP results) but for the selection of Best30 based on ranking the projection members with least root mean square error. Stipplings indicate regions where the results are statistically not significant at 95% confidence level.

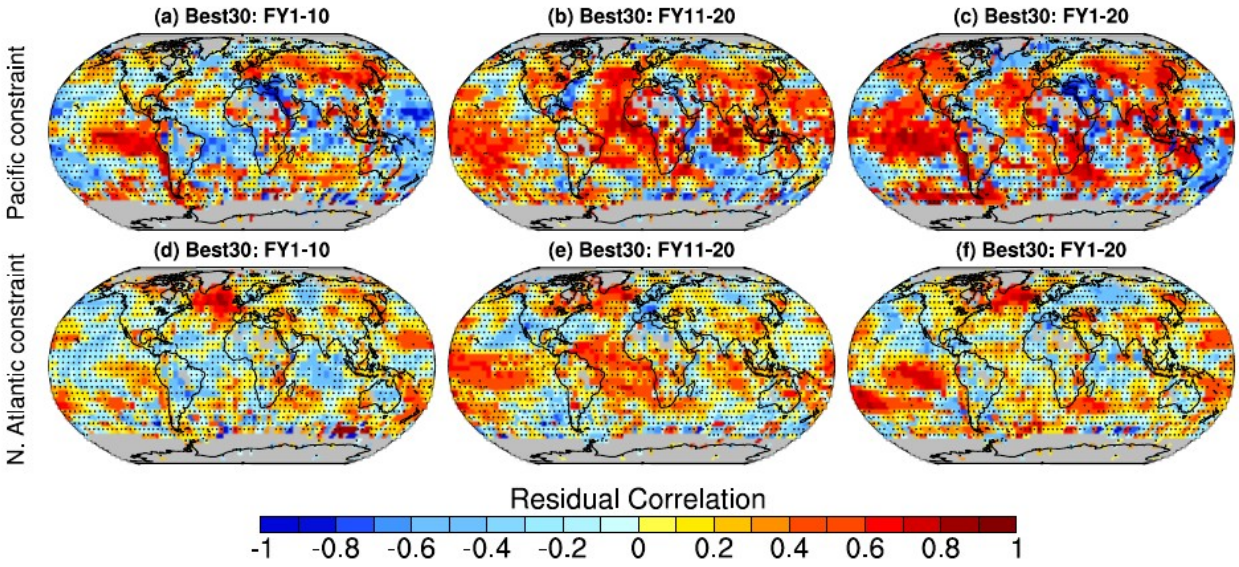

Figure S11: Residual correlations for near-surface temperature in the Best30 ensemble means constrained by nine year average SST anomaly patterns in the Pacific basin (a-c) and in the North Atlantic basin (d-f). Stipplings indicate regions where the results are statistically not significant at 95% confidence level.

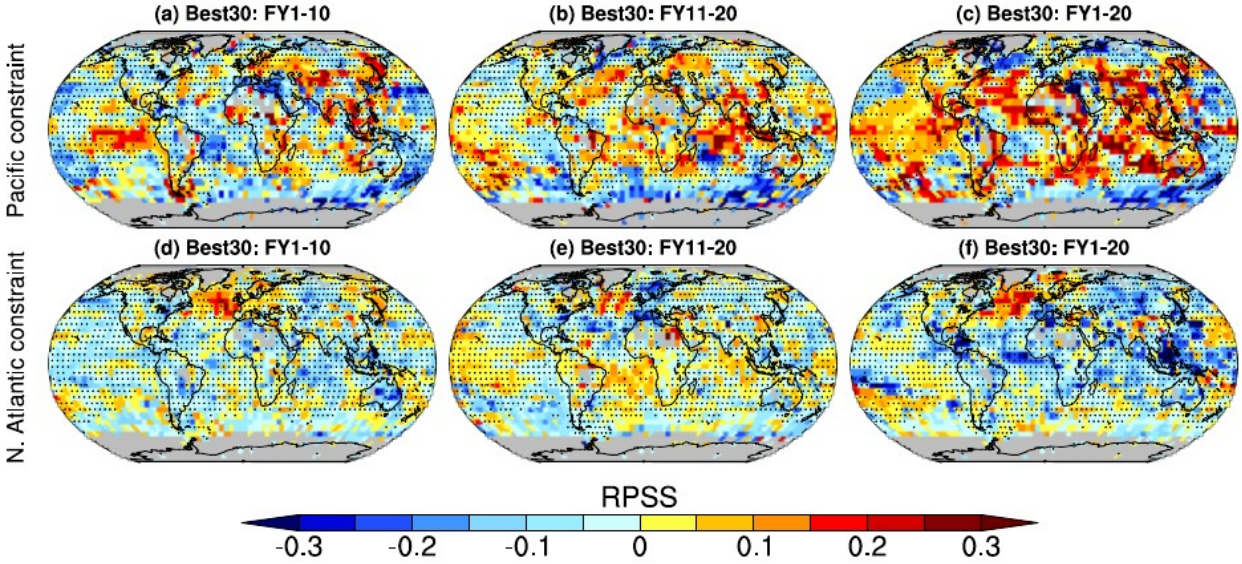

Figure S12: RPSS for Best30 ensemble near-surface temperature against the unconstrained CMIP6 ensemble of 212 members as reference. Best30 is constrained by nine year average SST anomaly patterns in the Pacific basin (a-c) and in the North Atlantic basic (d-f). Stipplings indicate regions where the results are statistically not significant at 95% confidence level.

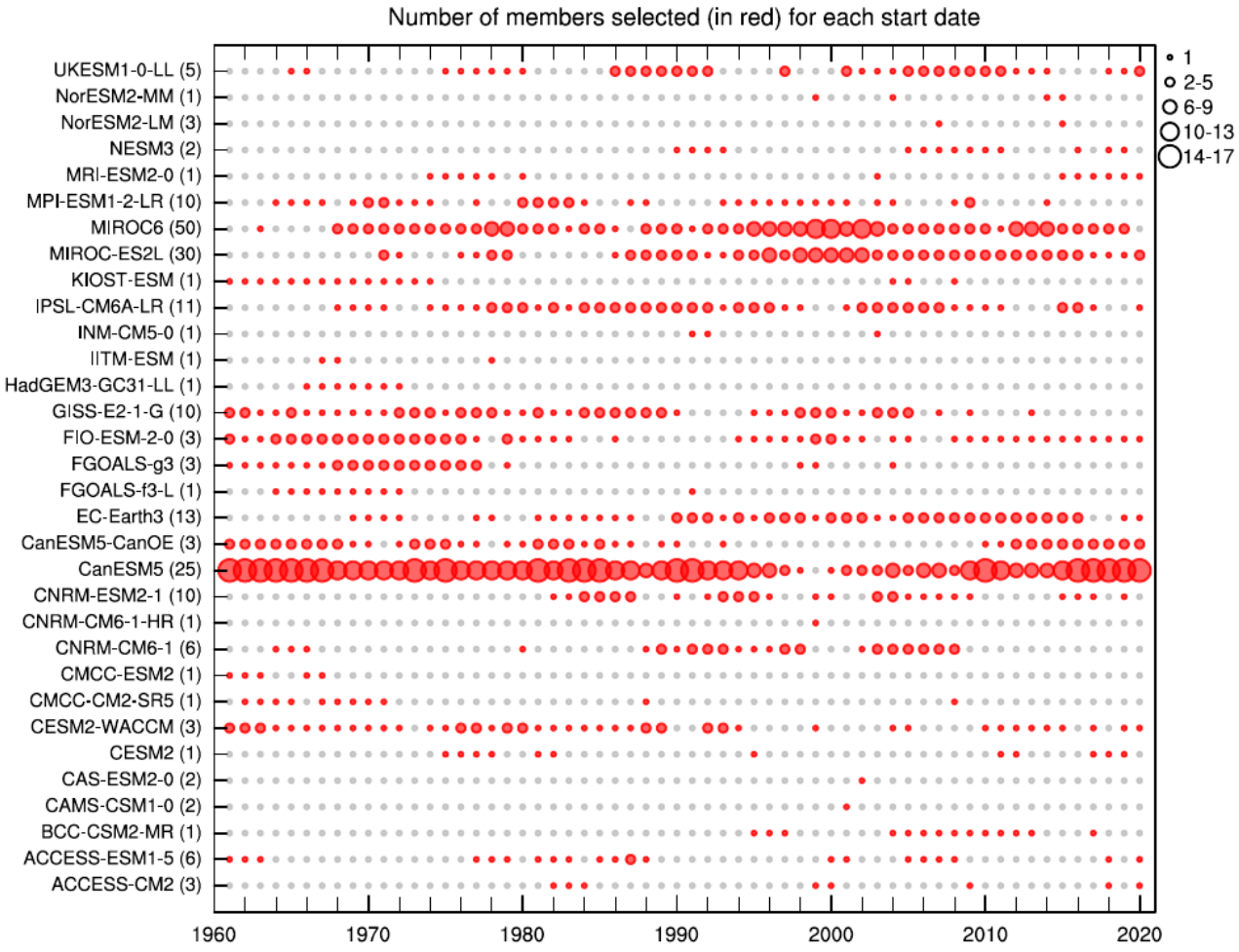

Figure S13: Count of how often each model is selected as part of the Best30 ensemble for each start date. The total number of ensemble members used are shown along with model names. The circle size indicates the count of how many ensemble members from each model are selected.

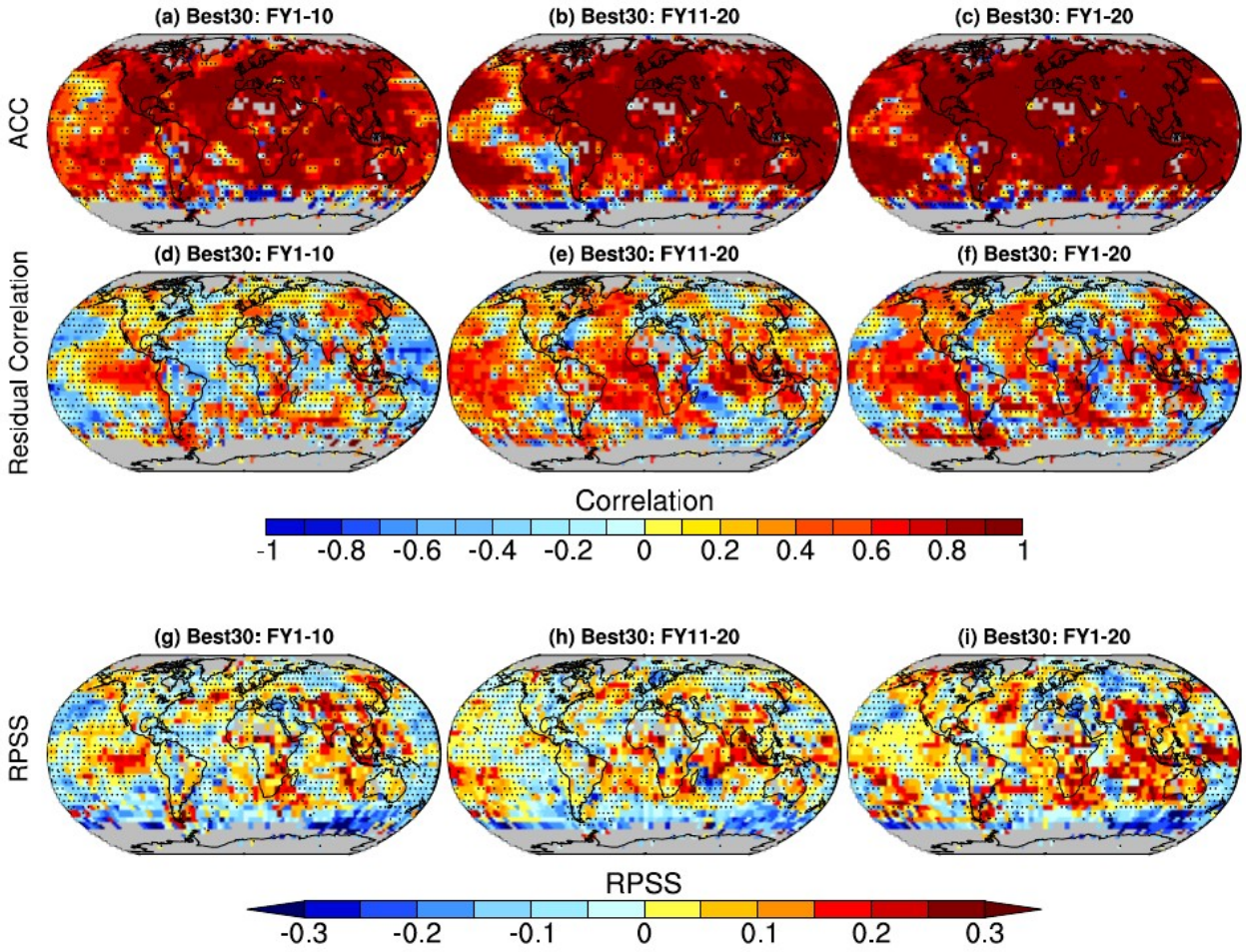

Figure S14: Same as Figure 2 (without DCPP results) but limiting the number of members for a model to be selected as part of Best30 to a maximum of 5. Anomaly correlation coefficient (ACC) between observed and predicted near-surface temperature anomalies for three forecast periods, average of forecast years 1-10, 11-20 and 1-20 (a-c). Residual correlations for Best30 (d-f) ensemble means after removing the forced signal (estimated based on ensemble mean of the unconstrained 212 members following Smith et al. (2019). RPSS for Best30 (g-i) against the unconstrained CMIP6 ensemble as reference. Stipplings indicate regions where the results are statistically not significant at 95% confidence level.

Text S1 Evaluating the hindcasts using different observational data sets.

This section evaluates the constrained ensembles and the DCPP using alternative observational reference data sets. For this we used surface air temperature from the Merged Land and Ocean Global Surface Temperature Analysis by NOAA (NOAAGlobalTemp, Huang et al., 2020), sea level pressure from the European Centre for Medium-Range Forecasts (ECMWF) Reanalysis Version 5 (ERA5; Hersbach et al., 2020) and precipitation data from the CRU TS 4.0.4 dataset (Harris et al., 2020). Overall the results shown in Figures S15-17 compare well with the results shown in the main text Figures 2-4. For example, for the surface temperature the Best30 ensemble shows high skill in terms of ACC and significant added value over the unconstrained ensemble in terms of residual correlations and RPSS in many global regions including the tropical Pacific, the Indian Ocean, north and south America and parts of Asian and Africa, (Figure S15). These results also suggest even higher added values than shown in Figure 2 especially over the southern Indian ocean with similar results for the Best30 and DCPP. The SLP and precipitation prediction skill of the constrained ensemble in Figures S16 and S17 respectively are generally similar to the results shown in Figures 3 and 4. The results based on these alternative observational datasets confirm the robustness of the skill of the constrained ensembles to the choice of reference dataset used for skill evaluation.

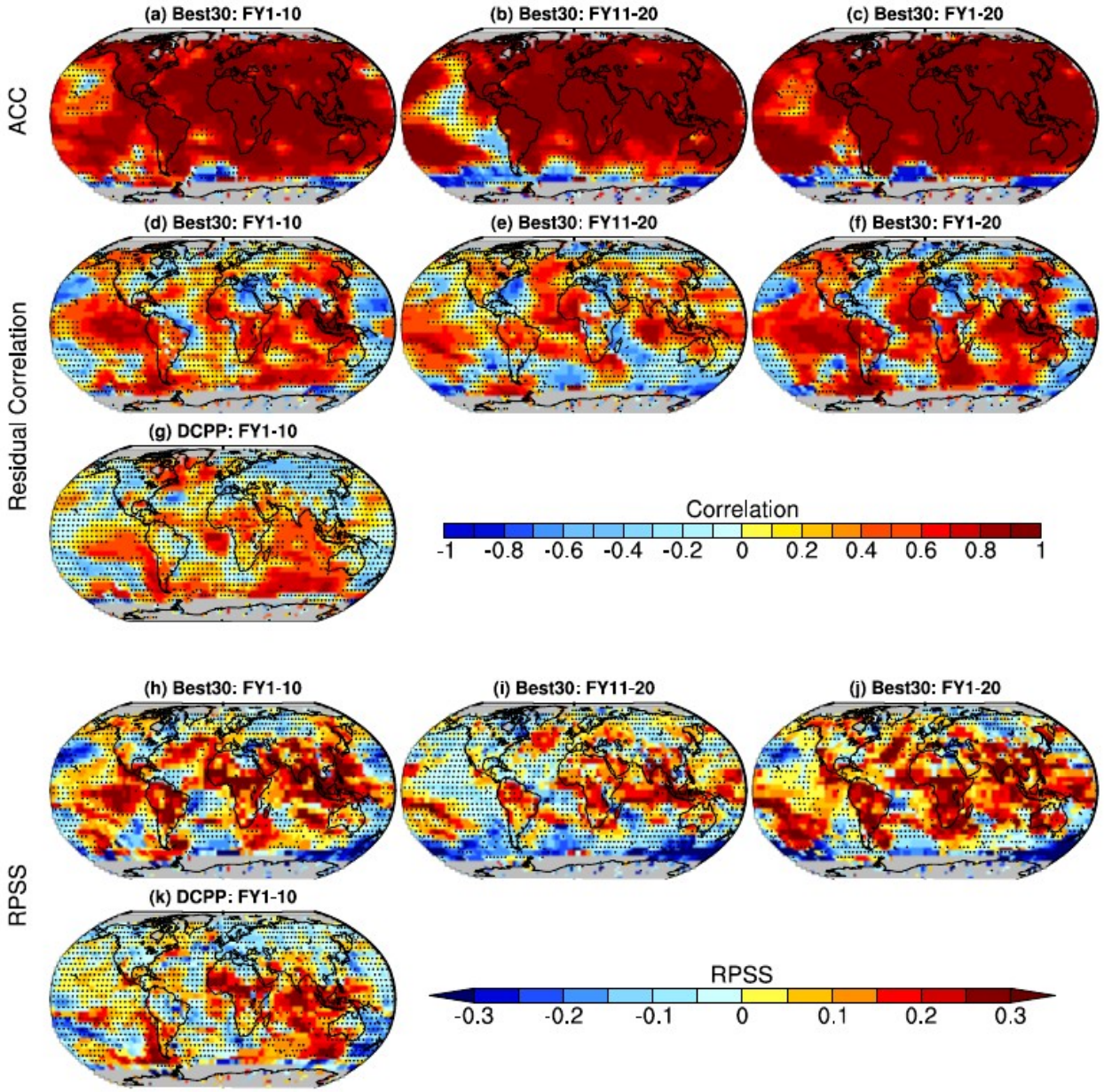

Figure S15: Same as Figure 2 but using NOAAGlobalTemp as observation. Anomaly correlation coefficient (ACC) between observed and predicted near-surface temperature anomalies for three forecast periods, average of forecast years 1-10, 11-20 and 1-20 (a-c). Residual correlations for Best30 (d-f) and for DCPP (g) ensemble means after removing the forced signal (estimated based on ensemble mean of the unconstrained CMIP6 212 members following Smith et al. (2019). RPSS for Best 30 (h-j) and for DCPP (k) against the unconstrained CMIP6 ensemble of 212 members as reference. Stipplings indicate regions where the results are statistically not significant at 95% confidence level.

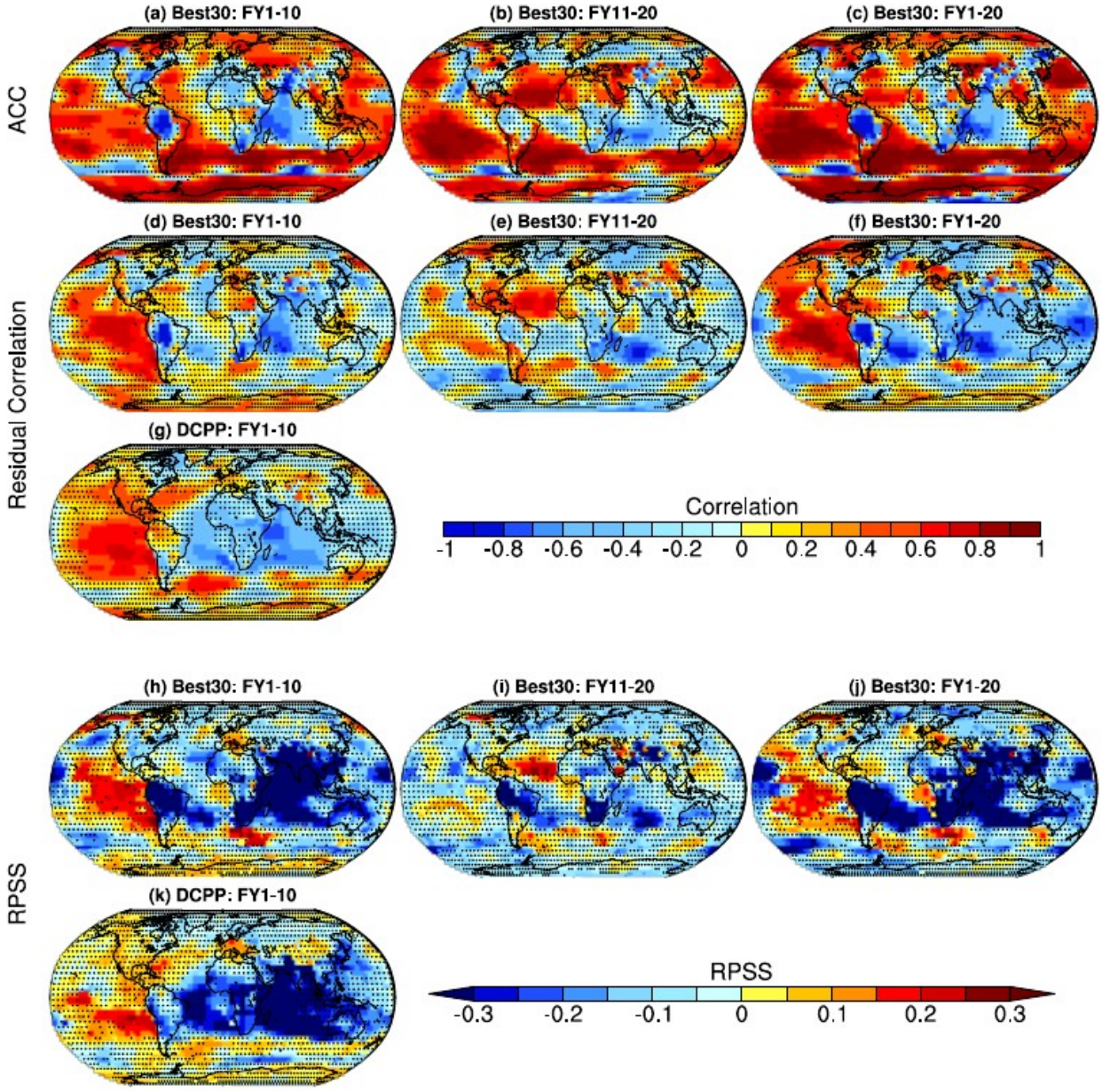

Figure S16: Same as Figure 3 but using ERA5 SLP. Anomaly correlation coefficient (ACC) between observed and predicted SLP anomalies for three forecast periods, average of forecast years 1-10, 11-20 and 1-20 (a-c). Residual correlations for Best30 (d-f) and for DCPP (g) ensemble means after removing the forced signal (estimated based on ensemble mean of the unconstrained 212 members following Smith et al. (2019). RPSS for Best30 (h-j) and for DCPP (k) against the unconstrained CMIP6 ensemble as reference. Stipplings indicate regions where the results are statistically not significant at 95% confidence level.

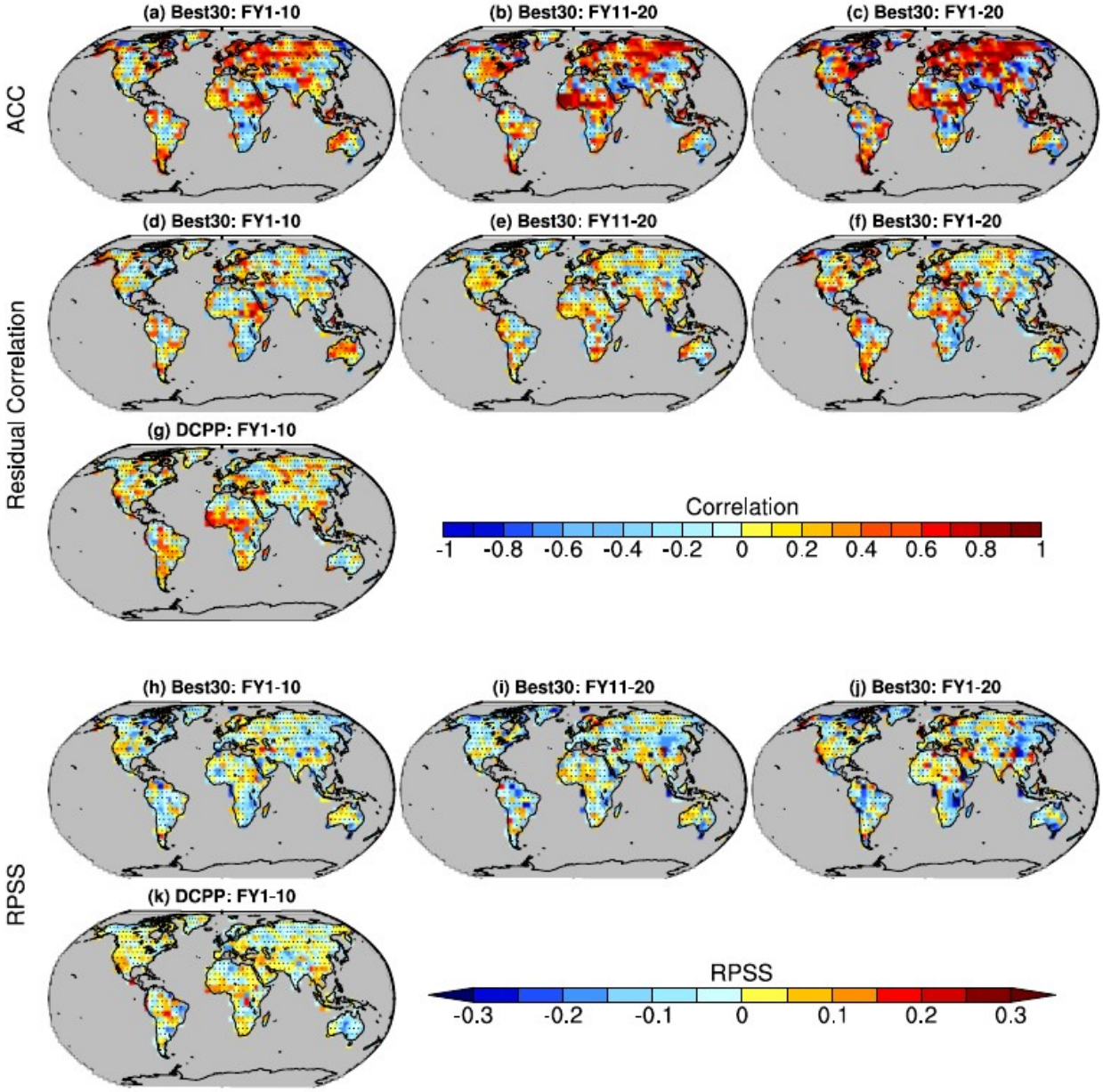

Figure S17: Same as Figure 4 but using CRU precipitation. Anomaly correlation coefficient (ACC) between observed and predicted precipitation anomalies for three forecast periods, average of forecast years 1-10, 11-20 and 1-20 (a-c). Residual correlations for Best30 (d-f) and for DCPP (g) ensemble means after removing the forced signal (estimated based on ensemble mean of the unconstrained 212 members following Smith et al. (2019). RPSS for Best30 (h-j) and for DCPP (k) against the unconstrained CMIP6 ensemble as reference. Stipplings indicate regions where the results are statistically not significant at 95% confidence level.

References

Andrews, M. B., Ridley, J. K., Wood, R. A., Andrews, T., Blockley, E. W., Booth, B., Burke, E., Dittus, A. J., Florek, P., Gray, L. J., Haddad, S., Hardiman, S. C., Hermanson, L., Hodson, D., Hogan, E., Jones, G. S., Knight, J. R., Kuhlbrodt, T., Misios, S., Mizielinski, M. S., Ringer, M. A., Robson, J., and Sutton, R. T.: Historical Simulations With HadGEM3-GC3.1 for CMIP6, J. Adv. Model. Earth Syst., 12, https://doi.org/10.1029/2019MS001995, 2020.

Bao, Y., Song, Z., and Qiao, F.: FIO-ESM Version 2.0: Model Description and Evaluation, J. Geophys. Res. Oceans, 125, https://doi.org/10.1029/2019JC016036, 2020.

Bethke, I., Wang, Y., Counillon, F., Keenlyside, N., Kimmritz, M., Fransner, F., Samuelsen, A., Langehaug, H., Svendsen, L., Chiu, P.-G., Passos, L., Bentsen, M., Guo, C., Gupta, A., Tjiputra, J., Kirkevåg, A., Olivié, D., Seland, Ø., Solsvik Vågane, J., Fan, Y., and Eldevik, T.: NorCPM1 and its contribution to CMIP6 DCPP, Geosci. Model Dev., 14, 7073–7116, https://doi.org/10.5194/gmd-14-7073-2021, 2021.

Bi, D., Dix, M., Marsland, S., O'Farrell, S., Sullivan, A., Bodman, R., Law, R., Harman, I., Srbinovsky, J., Rashid, H. A., Dobrohotoff, P., Mackallah, C., Yan, H., Hirst, A., Savita, A., Dias, F. B., Woodhouse, M., Fiedler, R., and Heerdegen, A.: Configuration and spin-up of ACCESS-CM2, the new generation Australian Community Climate and Earth System Simulator Coupled Model, JSHESS, 70, 225, https://doi.org/10.1071/ES19040, 2020.

Bilbao, R., Wild, S., Ortega, P., Acosta-Navarro, J., Arsouze, T., Bretonnière, P.-A., Caron, L.-P., Castrillo, M., Cruz-García, R., Cvijanovic, I., Doblas-Reyes, F. J., Donat, M., Dutra, E., Echevarría, P., Ho, A.-C., Loosveldt-Tomas, S., Moreno-Chamarro, E., Pérez-Zanon, N., Ramos, A., Ruprich-Robert, Y., Sicardi, V., Tourigny, E., and Vegas-Regidor, J.: Assessment of a full-field initialized decadal climate prediction system with the CMIP6 version of EC-Earth, Earth Syst. Dynam., 12, 173–196, https://doi.org/10.5194/esd-12-173-2021, 2021.

Boucher, O., Servonnat, J., Albright, A. L., Aumont, O., Balkanski, Y., Bastrikov, V., Bekki, S., Bonnet, R., Bony, S., Bopp, L., Braconnot, P., Brockmann, P., Cadule, P., Caubel, A., Cheruy, F., Codron, F., Cozic, A., Cugnet, D., D'Andrea, F., Davini, P., Lavergne, C., Denvil, S., Deshayes, J., Devilliers, M., Ducharne, A., Dufresne, J., Dupont, E., Éthé, C., Fairhead, L., Falletti, L., Flavoni, S., Foujols, M., Gardoll, S., Gastineau, G., Ghattas, J., Grandpeix, J., Guenet, B., Guez, L., E., Guilyardi, E., Guimberteau, M., Hauglustaine, D., Hourdin, F., Idelkadi,

A., Joussaume, S., Kageyama, M., Khodri, M., Krinner, G., Lebas, N., Levavasseur, G., Lévy, C., Li, L., Lott, F., Lurton, T., Luyssaert, S., Madec, G., Madeleine, J., Maignan, F., Marchand, M., Marti, O., Mellul, L., Meurdesoif, Y., Mignot, J., Musat, I., Ottlé, C., Peylin, P., Planton, Y., Polcher, J., Rio, C., Rochetin, N., Rousset, C., Sepulchre, P., Sima, A., Swingedouw, D., Thiéblemont, R., Traore, A. K., Vancoppenolle, M., Vial, J., Vialard, J., Viovy, N., and Vuichard, N.: Presentation and Evaluation of the IPSL-CM6A-LR Climate Model, J. Adv. Model. Earth Syst., 12, https://doi.org/10.1029/2019MS002010, 2020.

Cao, J., Wang, B., Yang, Y.-M., Ma, L., Li, J., Sun, B., Bao, Y., He, J., Zhou, X., and Wu, L.: The NUIST Earth System Model (NESM) version 3: description and preliminary evaluation, Geosci. Model Dev., 11, 2975–2993, https://doi.org/10.5194/gmd-11-2975-2018, 2018.

Cherchi, A., Fogli, P. G., Lovato, T., Peano, D., Iovino, D., Gualdi, S., Masina, S., Scoccimarro, E., Materia, S., Bellucci, A., and Navarra, A.: Global mean climate and main patterns of variability in the CMCC-CM2 coupled model, J. Adv. Model. Earth Syst., 2018MS001369, https://doi.org/10.1029/2018MS001369, 2018.

Christian, J. R., Denman, K. L., Hayashida, H., Holdsworth, A. M., Lee, W. G., Riche, O. G. J., Shao, A. E., Steiner, N., and Swart, N. C.: Ocean biogeochemistry in the Canadian Earth System Model version 5.0.3: CanESM5 and CanESM5-CanOE, Geoscientific Model Development, 15(11), 4393–4424. https://doi.org/10.5194/gmd-15-4393-2022, 2022.

Danabasoglu, G., Lamarque, J. -F., Bacmeister, J., Bailey, D. A., DuVivier, A. K., Edwards, J., Emmons, L. K., Fasullo, J., Garcia, R., Gettelman, A., Hannay, C., Holland, M. M., Large, W. G., Lauritzen, P. H., Lawrence, D. M., Lenaerts, J. T. M., Lindsay, K., Lipscomb, W. H., Mills, M. J., Neale, R., Oleson, K. W., Otto-Bliesner, B., Phillips, A. S., Sacks, W., Tilmes, S., Kampenhout, L., Vertenstein, M., Bertini, A., Dennis, J., Deser, C., Fischer, C., Fox-Kemper, B., Kay, J. E., Kinnison, D., Kushner, P. J., Larson, V. E., Long, M. C., Mickelson, S., Moore, J. K., Nienhouse, E., Polvani, L., Rasch, P. J., and Strand, W. G.: The Community Earth System Model Version 2 (CESM2), J. Adv. Model. Earth Syst., 12, https://doi.org/10.1029/2019MS001916, 2020.

Gettelman, A., Mills, M. J., Kinnison, D. E., Garcia, R. R., Smith, A. K., Marsh, D. R., Tilmes, S., Vitt, F., Bardeen, C. G., McInerny, J., Liu, H. -L., Solomon, S. C., Polvani, L. M., Emmons, L. K., Lamarque, J. -F., Richter, J. H., Glanville, A. S., Bacmeister, J. T., Phillips, A. S., Neale, R. B., Simpson, I. R., DuVivier, A. K., Hodzic, A., and Randel, W. J.: The Whole Atmosphere Community Climate Model Version 6 (WACCM6), JGR Atmospheres, 124, 12380–12403,

https://doi.org/10.1029/2019JD030943, 2019.

Guangqing, Z., Yunquan, Z., Jinrong, J., He, Z., Baodong, W., Hang, C., Tianyi, W., Huiqun, H., Jiawen, Z., Liang, Y., and Minghua, Z.: Earth System Model: CAS-ESM[J], Frontiers of Data and Computing, 2(1), 38-54, https://doi.org/10.11871/jfdc.issn.2096-742X.2020.01.004, 2020.

Hajima, T., Watanabe, M., Yamamoto, A., Tatebe, H., Noguchi, M. A., Abe, M., Ohgaito, R., Ito, A., Yamazaki, D., Okajima, H., Ito, A., Takata, K., Ogochi, K., Watanabe, S., and Kawamiya, M.: Development of the MIROC-ES2L Earth system model and the evaluation of biogeochemical processes and feedbacks, Geosci. Model Dev., 13, 2197–2244, https://doi.org/10.5194/gmd-13-2197-2020, 2020.

Harris, I., Osborn, T. J., Jones, P., and Lister, D.: Version 4 of the CRU TS monthly high-resolution gridded multivariate climate dataset, Sci Data, 7, 109, https://doi.org/10.1038/s41597-020-0453-3, 2020.

He, B., Yu, Y., Bao, Q., Lin, P., Liu, H., Li, J., Wang, L., Liu, Y., Wu, G., Chen, K., Guo, Y., Zhao, S., Zhang, X., Song, M., and Xie, J.: CAS FGOALS-f3-L model dataset descriptions for CMIP6 DECK experiments, Atmospheric and Oceanic Science Letters, 13, 582–588, https://doi.org/10.1080/16742834.2020.1778419, 2020.

Hersbach, H., Bell, B., Berrisford, P., Hirahara, S., Horányi, A., Muñoz-Sabater, J., Nicolas, J., Peubey, C., Radu, R., Schepers, D., Simmons, A., Soci, C., Abdalla, S., Abellan, X., Balsamo, G., Bechtold, P., Biavati, G., Bidlot, J., Bonavita, M., Chiara, G., Dahlgren, P., Dee, D., Diamantakis, M., Dragani, R., Flemming, J., Forbes, R., Fuentes, M., Geer, A., Haimberger, L., Healy, S., Hogan, R. J., Hólm, E., Janisková, M., Keeley, S., Laloyaux, P., Lopez, P., Lupu, C., Radnoti, G., Rosnay, P., Rozum, I., Vamborg, F., Villaume, S., and Thépaut, J.: The ERA5 global reanalysis, Q.J.R. Meteorol. Soc., 146, 1999–2049, https://doi.org/10.1002/qj.3803, 2020.

Huang, B., Menne, M. J., Boyer, T., Freeman, E., Gleason, B. E., Lawrimore, J. H., Liu, C., Rennie, J. J., Schreck, C. J., Sun, F., Vose, R., Williams, C. N., Yin, X., and Zhang, H.-M.: Uncertainty Estimates for Sea Surface Temperature and Land Surface Air Temperature in NOAAGlobalTemp Version 5, 33, 1351–1379, https://doi.org/10.1175/JCLI-D-19-0395.1, 2020.

Kelley, M., Schmidt, G. A., Nazarenko, L. S., Bauer, S. E., Ruedy, R., Russell, G. L., Ackerman, A. S., Aleinov, I., Bauer, M., Bleck, R., Canuto, V., Cesana, G., Cheng, Y., Clune, T. L., Cook, B. I., Cruz, C. A., Del Genio, A. D., Elsaesser, G. S., Faluvegi, G., Kiang, N. Y., Kim, D., Lacis,

A. A., Leboissetier, A., LeGrande, A. N., Lo, K. K., Marshall, J., Matthews, E. E., McDermid, S., Mezuman, K., Miller, R. L., Murray, L. T., Oinas, V., Orbe, C., García-Pando, C. P., Perlwitz, J. P., Puma, M. J., Rind, D., Romanou, A., Shindell, D. T., Sun, S., Tausnev, N., Tsigaridis, K., Tselioudis, G., Weng, E., Wu, J., and Yao, M.: GISS-E2.1: Configurations and Climatology, J. Adv. Model. Earth Syst., 12, https://doi.org/10.1029/2019MS002025, 2020.

Krishnan, R., Swapna, P., Vellore, R., Narayanasetti, S., Prajeesh, A. G., Choudhury, A. D., Singh, M., Sabin, T. P., and Sanjay, J.: The IITM Earth System Model (ESM): Development and Future Roadmap, in: Current Trends in the Representation of Physical Processes in Weather and Climate Models, edited by: Randall, D. A., Srinivasan, J., Nanjundiah, R. S., and Mukhopadhyay, P., Springer Singapore, Singapore, 183–195, https://doi.org/10.1007/978-981-13-3396-5_9, 2019.

Lovato, T., Peano, D., Butenschön, M., Materia, S., Iovino, D., Scoccimarro, E., Fogli, P. G., Cherchi, A., Bellucci, A., Gualdi, S., Masina, S., and Navarra, A.: CMIP6 Simulations With the CMCC Earth System Model (CMCC-ESM2), J Adv Model Earth Syst, 14, https://doi.org/10.1029/2021MS002814, 2022.

Mauritsen, T., Bader, J., Becker, T., Behrens, J., Bittner, M., Brokopf, R., Brovkin, V., Claussen, M., Crueger, T., Esch, M., Fast, I., Fiedler, S., Fläschner, D., Gayler, V., Giorgetta, M., Goll, D. S., Haak, H., Hagemann, S., Hedemann, C., Hohenegger, C., Ilyina, T., Jahns, T., Jimenéz-de-la-Cuesta, D., Jungclaus, J., Kleinen, T., Kloster, S., Kracher, D., Kinne, S., Kleberg, D., Lasslop, G., Kornblueh, L., Marotzke, J., Matei, D., Meraner, K., Mikolajewicz, U., Modali, K., Möbis, B., Müller, W. A., Nabel, J. E. M. S., Nam, C. C. W., Notz, D., Nyawira, S., Paulsen, H., Peters, K., Pincus, R., Pohlmann, H., Pongratz, J., Popp, M., Raddatz, T. J., Rast, S., Redler, R., Reick, C. H., Rohrschneider, T., Schemann, V., Schmidt, H., Schnur, R., Schulzweida, U., Six, K. D., Stein, L., Stemmler, I., Stevens, B., Storch, J., Tian, F., Voigt, A., Vrese, P., Wieners, K., Wilkenskjeld, S., Winkler, A., and Roeckner, E.: Developments in the MPI-M Earth System Model version 1.2 (MPI-ESM1.2) and Its Response to Increasing CO_2, J. Adv. Model. Earth Syst., 11, 998–1038, https://doi.org/10.1029/2018MS001400, 2019.

Müller, W. A., Jungclaus, J. H., Mauritsen, T., Baehr, J., Bittner, M., Budich, R., Bunzel, F., Esch, M., Ghosh, R., Haak, H., Ilyina, T., Kleine, T., Kornblueh, L., Li, H., Modali, K., Notz, D., Pohlmann, H., Roeckner, E., Stemmler, I., Tian, F., and Marotzke, J.: A Higher-resolution Version of the Max Planck Institute Earth System Model (MPI-ESM1.2-HR), J. Adv. Model. Earth Syst., 10, 1383–1413, https://doi.org/10.1029/2017MS001217, 2018.

Pak, G., Noh, Y., Lee, M.-I., Yeh, S.-W., Kim, D., Kim, S.-Y., Lee, J.-L., Lee, H. J., Hyun, S.-H., Lee, K.-Y., Lee, J.-H., Park, Y.-G., Jin, H., Park, H., and Kim, Y. H.: Korea Institute of Ocean Science and Technology Earth System Model and Its Simulation Characteristics, Ocean Sci. J., 56, 18–45, https://doi.org/10.1007/s12601-021-00001-7, 2021.

Pu, Y., Liu, H., Yan, R., Yang, H., Xia, K., Li, Y., Dong, L., Li, L., Wang, H., Nie, Y., Song, M., Xie, J., Zhao, S., Chen, K., Wang, B., Li, J., and Zuo, L.: CAS FGOALS-g3 Model Datasets for the CMIP6 Scenario Model Intercomparison Project (ScenarioMIP), Adv. Atmos. Sci., 37, 1081–1092, https://doi.org/10.1007/s00376-020-2032-0, 2020.

Rong, X. Y., Li J., Chen, H. M., Xin, Y. F., Su, J. Z., Hua, L. J., and Zhang Z. Q.: Introduction of CAMS-CSM model and its participation in CMIP6, Climate Change Research, 15(5), 540-544, https://doi.org/10.12006/j.issn.1673-1719.2019.186, 2019.

Séférian, R., Nabat, P., Michou, M., Saint-Martin, D., Voldoire, A., Colin, J., Decharme, B., Delire, C., Berthet, S., Chevallier, M., Sénési, S., Franchisteguy, L., Vial, J., Mallet, M., Joetzjer, E., Geoffroy, O., Guérémy, J., Moine, M., Msadek, R., Ribes, A., Rocher, M., Roehrig, R., Salas-y-Mélia, D., Sanchez, E., Terray, L., Valcke, S., Waldman, R., Aumont, O., Bopp, L., Deshayes, J., Éthé, C., and Madec, G.: Evaluation of CNRM Earth System Model, CNRM-ESM2-1: Role of Earth System Processes in Present-Day and Future Climate, J. Adv. Model. Earth Syst., 11, 4182–4227, https://doi.org/10.1029/2019MS001791, 2019.

Seland, Ø., Bentsen, M., Olivié, D., Toniazzo, T., Gjermundsen, A., Graff, L. S., Debernard, J. B., Gupta, A. K., He, Y.-C., Kirkevåg, A., Schwinger, J., Tjiputra, J., Aas, K. S., Bethke, I., Fan, Y., Griesfeller, J., Grini, A., Guo, C., Ilicak, M., Karset, I. H. H., Landgren, O., Liakka, J., Moseid, K. O., Nummelin, A., Spensberger, C., Tang, H., Zhang, Z., Heinze, C., Iversen, T., and Schulz, M.: Overview of the Norwegian Earth System Model (NorESM2) and key climate response of CMIP6 DECK, historical, and scenario simulations, Geosci. Model Dev., 13, 6165–6200, https://doi.org/10.5194/gmd-13-6165-2020, 2020.

Sellar, A. A., Jones, C. G., Mulcahy, J. P., Tang, Y., Yool, A., Wiltshire, A., O'Connor, F. M., Stringer, M., Hill, R., Palmieri, J., Woodward, S., Mora, L., Kuhlbrodt, T., Rumbold, S. T., Kelley, D. I., Ellis, R., Johnson, C. E., Walton, J., Abraham, N. L., Andrews, M. B., Andrews, T., Archibald, A. T., Berthou, S., Burke, E., Blockley, E., Carslaw, K., Dalvi, M., Edwards, J., Folberth, G. A., Gedney, N., Griffiths, P. T., Harper, A. B., Hendry, M. A., Hewitt, A. J., Johnson, B., Jones, A., Jones, C. D., Keeble, J., Liddicoat, S., Morgenstern, O., Parker, R. J., Predoi, V., Robertson, E., Siahaan, A., Smith, R. S., Swaminathan, R., Woodhouse, M. T., Zeng, G., and

Zerroukat, M.: UKESM1: Description and Evaluation of the U.K. Earth System Model, J. Adv. Model. Earth Syst., 11, 4513–4558, https://doi.org/10.1029/2019MS001739, 2019.

Sellar, A. A., Walton, J., Jones, C. G., Wood, R., Abraham, N. L., Andrejczuk, M., Andrews, M. B., Andrews, T., Archibald, A. T., Mora, L., Dyson, H., Elkington, M., Ellis, R., Florek, P., Good, P., Gohar, L., Haddad, S., Hardiman, S. C., Hogan, E., Iwi, A., Jones, C. D., Johnson, B., Kelley, D. I., Kettleborough, J., Knight, J. R., Köhler, M. O., Kuhlbrodt, T., Liddicoat, S., Linova-Pavlova, I., Mizielinski, M. S., Morgenstern, O., Mulcahy, J., Neininger, E., O'Connor, F. M., Petrie, R., Ridley, J., Rioual, J., Roberts, M., Robertson, E., Rumbold, S., Seddon, J., Shepherd, H., Shim, S., Stephens, A., Teixiera, J. C., Tang, Y., Williams, J., Wiltshire, A., and Griffiths, P. T.: Implementation of U.K. Earth System Models for CMIP6, J. Adv. Model. Earth Syst., 12, https://doi.org/10.1029/2019MS001946, 2020.

Swart, N. C., Cole, J. N. S., Kharin, V. V., Lazare, M., Scinocca, J. F., Gillett, N. P., Anstey, J., Arora, V., Christian, J. R., Hanna, S., Jiao, Y., Lee, W. G., Majaess, F., Saenko, O. A., Seiler, C., Seinen, C., Shao, A., Sigmond, M., Solheim, L., von Salzen, K., Yang, D., and Winter, B.: The Canadian Earth System Model version 5 (CanESM5.0.3), Geosci. Model Dev., 12, 4823–4873, https://doi.org/10.5194/gmd-12-4823-2019, 2019.

Tatebe, H., Ogura, T., Nitta, T., Komuro, Y., Ogochi, K., Takemura, T., Sudo, K., Sekiguchi, M., Abe, M., Saito, F., Chikira, M., Watanabe, S., Mori, M., Hirota, N., Kawatani, Y., Mochizuki, T., Yoshimura, K., Takata, K., O'ishi, R., Yamazaki, D., Suzuki, T., Kurogi, M., Kataoka, T., Watanabe, M., and Kimoto, M.: Description and basic evaluation of simulated mean state, internal variability, and climate sensitivity in MIROC6, Geosci. Model Dev., 12, 2727–2765, https://doi.org/10.5194/gmd-12-2727-2019, 2019.

Voldoire, A., Saint-Martin, D., Sénési, S., Decharme, B., Alias, A., Chevallier, M., Colin, J., Guérémy, J. -F., Michou, M., Moine, M. -P., Nabat, P., Roehrig, R., Salas y Mélia, D., Séférian, R., Valcke, S., Beau, I., Belamari, S., Berthet, S., Cassou, C., Cattiaux, J., Deshayes, J., Douville, H., Ethé, C., Franchistéguy, L., Geoffroy, O., Lévy, C., Madec, G., Meurdesoif, Y., Msadek, R., Ribes, A., Sanchez-Gomez, E., Terray, L., and Waldman, R.: Evaluation of CMIP6 DECK Experiments With CNRM-CM6-1, J. Adv. Model. Earth Syst., 11, 2177–2213, https://doi.org/10.1029/2019MS001683, 2019.

Volodin, E. M., Mortikov, E. V., Kostrykin, S. V., Galin, V. Ya., Lykossov, V. N., Gritsun, A. S., Diansky, N. A., Gusev, A. V., and Iakovlev, N. G.: Simulation of the present-day climate with the climate model INMCM5, Clim Dyn, 49, 3715–3734, https://doi.org/10.1007/s00382-017-3539-7,

2017.

Wu, T., Lu, Y., Fang, Y., Xin, X., Li, L., Li, W., Jie, W., Zhang, J., Liu, Y., Zhang, L., Zhang, F., Zhang, Y., Wu, F., Li, J., Chu, M., Wang, Z., Shi, X., Liu, X., Wei, M., Huang, A., Zhang, Y., and Liu, X.: The Beijing Climate Center Climate System Model (BCC-CSM): the main progress from CMIP5 to CMIP6, Geosci. Model Dev., 12, 1573–1600, https://doi.org/10.5194/gmd-12-1573-2019, 2019.

Yukimoto, S., Kawai, H., Koshiro, T., Oshima, N., Yoshida, K., Urakawa, S., Tsujino, H., Deushi, M., Tanaka, T., Hosaka, M., Yabu, S., Yoshimura, H., Shindo, E., Mizuta, R., Obata, A., Adachi, Y., and Ishii, M.: The Meteorological Research Institute Earth System Model Version 2.0, MRI-ESM2.0: Description and Basic Evaluation of the Physical Component, Journal of the Meteorological Society of Japan, 97, 931–965, https://doi.org/10.2151/jmsj.2019-051, 2019.

Ziehn, T., Chamberlain, M. A., Law, R. M., Lenton, A., Bodman, R. W., Dix, M., Stevens, L., Wang, Y.-P., and Srbinovsky, J.: The Australian Earth System Model: ACCESS-ESM1.5, JSHESS, 70, 193, https://doi.org/10.1071/ES19035, 2020.